Chapter 16
Derivative-Less Arclength Control-Based Continuation for the Experimental Identification of Nonlinear Frequency Responses

Gaëtan Abeloos and Gaëtan Kerschen

Abstract This study focuses on the continuation process that is inherent to control-based continuation. Existing continuation procedures can be separated in two families. Similarly to numerical continuation, derivative-based methods find the solution of an objective function, the derivatives of which are estimated using finite differences. In mapping-based methods, the input parameter space is exhaustively or partially explored during the experiment. The features of interest can then be extracted during a post-processing phase or in parallel to the experiment. A novel arclength continuation procedure is developed in this paper. It requires neither the estimation of derivatives nor the identification of responses outside the features of interest, thus simplifying and accelerating the continuation process. The method is demonstrated numerically using a Duffing oscillator.

Keywords Nonlinear vibration · Control-based continuation · Arclength continuation · Duffing oscillator · Frequency responses

16.1 Arclength Continuation: The Basic Idea

The objective of this paper is to develop a continuation procedure which is simple to conceptualize and to implement and which avoids the need for post-processing or offline computations. The method is inspired by (i) the numerical arclength continuation procedure [1, 2], during which a control parameter is changed until it reaches the desired equilibrium, and (ii) the adaptive filtering-based online CBC experiment [3].

Because the sought frequency response curve (FRC) is one-dimensional in the input parameter space, a sufficiently small ellipse centered on the branch intersects it twice, as illustrated by the red markers in Fig. 16.1. One intersection is a previously identified response, and the other one is the next response to be identified. Successive responses on the FRC can thus be identified by increasing the arc angle α on the ellipse until the system reaches the next intersection. The response lies on the FRC if the excitation amplitude p given by the CBC controller equals the targeted excitation amplitude p^*. For illustration, Fig. 16.2 depicts the value of p depending on the arc angle α along the ellipse in Fig. 16.1. The ellipse intersects the FRC twice, because p reaches the target value p^* twice.

The continuation procedure is detailed in Fig. 16.3. We only need to know two responses on the FRC to identify a third one; the current one is denoted (Ω_c, X_c^*), and the previous one (Ω_p, X_p^*). An ellipse with semi-major axes $\Delta\Omega$ and ΔX_1^* is centered at the current point. The slope angle β between the current and previous points approximates the FRC slope. The input parameters (Ω, X_1^*) are set on the ellipse with an arc angle α from the previous point. The arc angle α is increased progressively from an initial angle α_0 sufficiently far away from the previous point until p reaches p^*, up to a certain tolerance tol_p.

In practice, we advise to identify the backbone curve before using the arclength continuation method to identify an FRC. In doing so, the experimenter can estimate the intervals in which the frequency and amplitude vary, and, in turn, adimentionalize the input parameter space (Ω, X_1^*) such that the eccentricity of the ellipse is close to unity, i.e., $\Delta\Omega \approx \Delta X_1^*$. Additionally, knowing the backbone allows to decrease the rate of change of the arclength when approaching the resonance peak, the region where transients can have the greatest effect on accuracy. The resonance peak can also be localized by looking at the evolution of the phase lag. An arc angle margin α_0 is chosen to ensure a sufficient distance with previously identified

G. Abeloos · G. Kerschen (✉)
Aerospace and Mechanical Engineering Department, University of Liège, Liège, Belgium
e-mail: gaetan.abeloos@uliege.be; g.kerschen@uliege.be

M. R. W. Brake et al. (eds.), *Nonlinear Structures & Systems, Volume 1*, Conference Proceedings
of the Society for Experimental Mechanics Series, https://doi.org/10.1007/978-3-031-36999-5_16

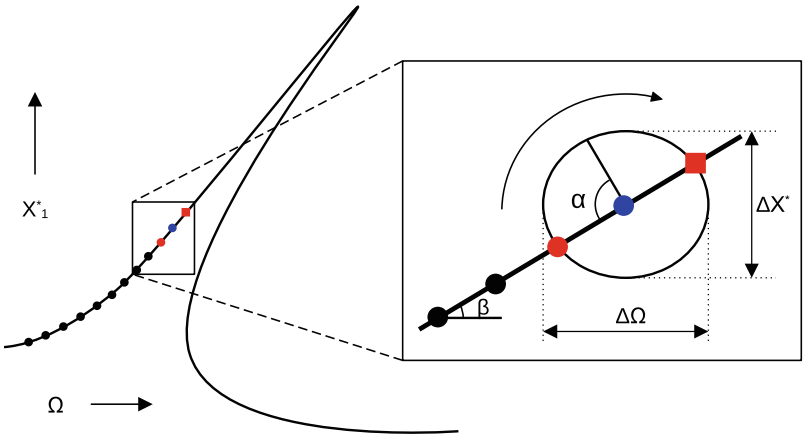

Fig. 16.1 The proposed arclength continuation procedure. Previously identified responses: circles; next response to be identified: square, center of the arc (blue) and responses on the arc (red)

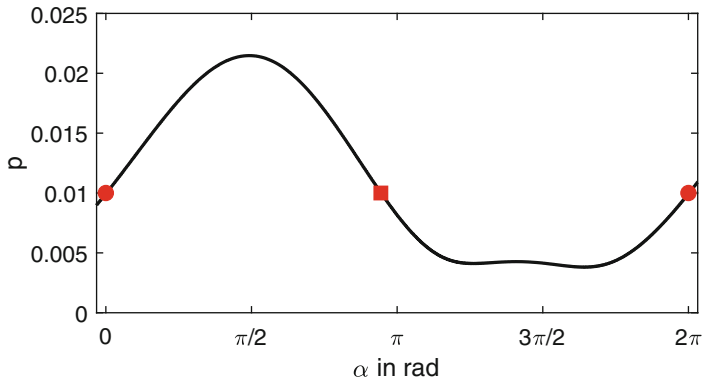

Fig. 16.2 Force amplitude p during the CBC experiment (Table 16.2) along the arc centered at $X^* = 0.02$, $\Omega = 40.8$ with the continuation parameters in Table 16.3 and excitation amplitude target $p^* = 0.01$. Previously identified response, circles, and next response: square

Algorithm 6.1 Arclength continuation for CBC experiment

1: $(\Omega_\mathrm{p}, X_\mathrm{p}^*)$ and $(\Omega_\mathrm{c}, X_\mathrm{c}^*)$ defined by user
2: **loop**
3: $\quad\alpha \leftarrow \alpha_0$
4: $\quad\beta \leftarrow \mathrm{atan2}(X_\mathrm{c}^* - X_\mathrm{p}^*, \Omega_\mathrm{c} - \Omega_\mathrm{p})$
5: $\quad(\Omega, X_1^*) = (\Omega_\mathrm{c} + \Delta\Omega\cos(\beta + \pi - \alpha), X_\mathrm{c}^* + \Delta X^* \sin(\beta + \pi - \alpha))$
6: $\quad$Wait a duration t_wait for steady state
7: $\quad$**while** $|p - p^*| > \mathrm{tol}_p$ **do**
8: $\quad\quad$Increase α with chosen method (see Section 6.4.1)
9: $\quad$**end while**
10: $\quad(\Omega_\mathrm{p}, X_\mathrm{p}^*) \leftarrow (\Omega_\mathrm{c}, X_\mathrm{c}^*)$
11: $\quad(\Omega_\mathrm{c}, X_\mathrm{c}^*) \leftarrow (\Omega, X_1^*)$
12: **end loop**

Fig. 16.3 Arclength continuation for CBC experiment

responses on the FRC. Finally, a cooldown time t_wait is needed for damping the transients resulting from sudden changes in input parameters.

16.2 Numerical Example

In this section, the arclength continuation method is demonstrated numerically using the Duffing oscillator in Table 16.1 with the parameters in Tables 16.2 and 16.3. N is the number of harmonics considered in the harmonic balance method used to calculate the reference FRCs, μ is the internal parameter of the adaptive filter, and k_d is the differential gain.

During a CBC experiment, the reference derivative $\dot{x}^*$ appears in the differential controller. It is usually equivalent to define the reference signal x^*, then differentiate it to obtain $\dot{x}^*$, or to define $\dot{x}^*$ directly. However, for arclength continuation, because the reference amplitude follows an ellipse in the input parameter space, the path is different if the fundamental amplitude of x^*, X_1^*, or the fundamental amplitude of $\dot{x}^*$, ΩX_1^*, is considered, especially when the frequency Ω changes significantly during the experiment. In this section, we implement the CBC experiment by defining $\dot{x}^*$ directly. The reference amplitudes are therefore displayed as ΩX_1^*.

Three strategies for moving along the ellipse and reaching the force target p^* are introduced. The first method is to sweep at a constant rate $\dot{\alpha} = \eta_\alpha$ until the excitation amplitude tolerance tol_p is reached. The path followed in the input parameter space is represented in Fig. 16.4. Figure 16.5 shows that the system is not in steady state when p^* is reached. Transients both in the system response and in the adaptive filters thus decrease the accuracy of the identified FRC, which is slightly shifted compared to the harmonic balance reference in Fig. 16.4.

The impact of changes in the sweep rate η_α or the semi-major axes $(\Delta\Omega, \Delta X^*)$ is plotted in Fig. 16.6. As expected, decreasing the sweep rate reduces the transients, which, in turn, increases the accuracy. However, this comes at the cost of a longer testing time (Table 16.4). When increasing the sweep rate, the more important transients may prevent the estimated force amplitude from reaching p^*. In this case, the continuation procedure is looping indefinitely and fails to go across the fold bifurcation. Reducing the size of the arc allows the experimenter to identify more points on the FRC, as confirmed in Fig. 16.6. Additionally, smaller arcs reduce the magnitude of the transients. Eventually, the accuracy is improved, whereas testing time is increased (Table 16.4).

Table 16.1 Parameters of the Duffing oscillator

m	c	k	$f_{\text{nl}}(x)$
0.05	0.2	57	$2 \times 10^8 x^3$

Table 16.2 Simulation parameters of the CBC experiment

N	f_s in kHz	μ	k_d
5	5	0.001	2

Table 16.3 CBC continuation parameters

tol_p	α_0	η_α	k_i	$\Delta\Omega$	ΔX^*	t_{wait}
$p^*/100$	$\pi/4$	$\pi/15$	75	0.5	0.002	2

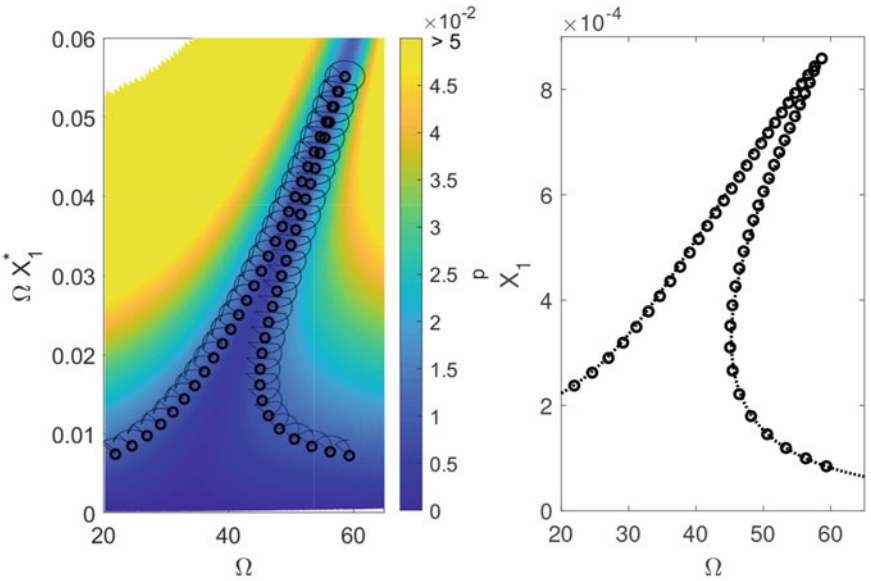

Fig. 16.4 Arclength continuation of a cubic oscillator with arclength sweep. The accepted points are marked by circles. (**a**) Input parameter space and (**b**) FRC at $p = 0.01$ (harmonic balance in dotted curve)

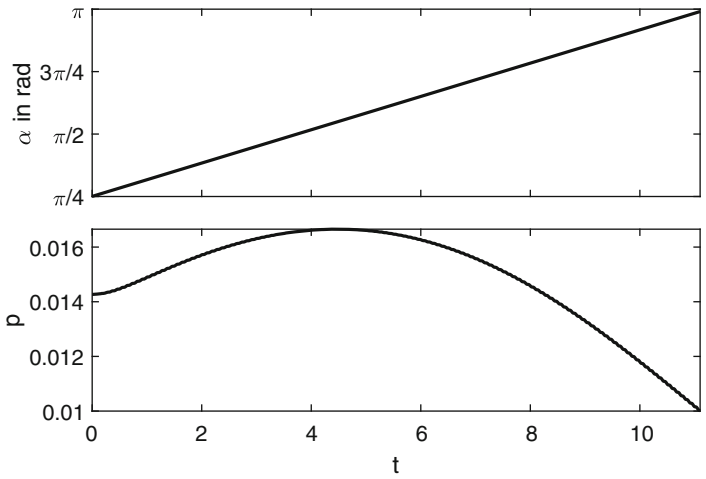

Fig. 16.5 Time series of the arc angle α (arc sweep) and force amplitude p along an arc centered at $\Omega X^* = 0.02$, $\Omega = 6.5$

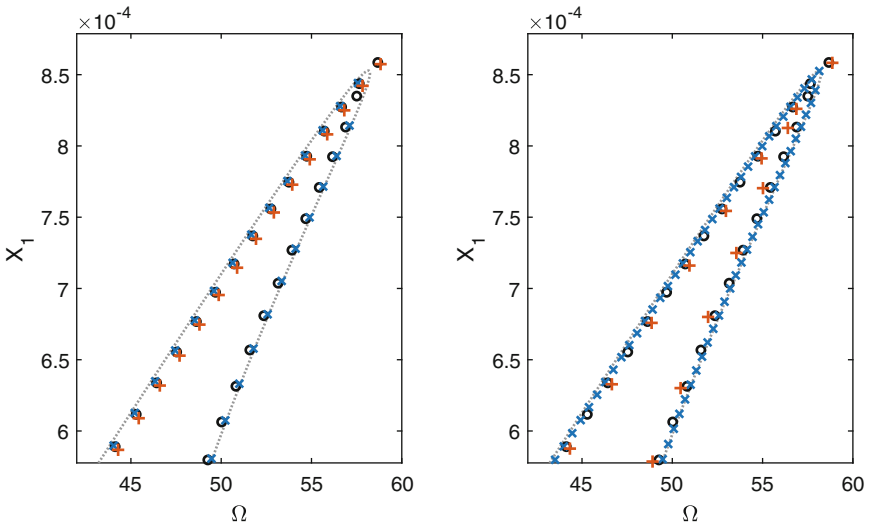

Fig. 16.6 Parametric study varying (**a**) the sweep rate $\eta_\alpha = \pi/30$ (blue $\times$), $\pi/15$ (black $\circ$), and $2\pi/15$ (orange $+$) or (**b**) the semi-major axes $(\Delta\Omega, \Delta X^*) = (0.25, 0.001)$ (blue $\times$), $(0.5, 0.002)$ (black $\circ$), and $(1, 0.004)$ (orange $+$). The dotted curve represents harmonic balance results

Table 16.4 Time (s) to reach the amplitude peak of the cubic oscillator

	Arc sweep	Arc control
Reference	365	259
Slower	650	500
Faster	*210	*153
Smaller arc	908	1486
Larger arc	180	*73

The reference parameters are $(\Delta\Omega, \Delta X^*) = (0.5, 0.002)$, $\eta_\alpha = \pi/30$, and $k_\mathrm{i} = 75$. The slower and faster runs correspond to $\eta_\alpha/2 - k_\mathrm{i}/2$ and $2\eta_\alpha - 2k_\mathrm{i}$, respectively. Smaller and larger arcs correspond to half and twice the reference semi-major axes. An asterisk means CBC failed to go across the fold bifurcation

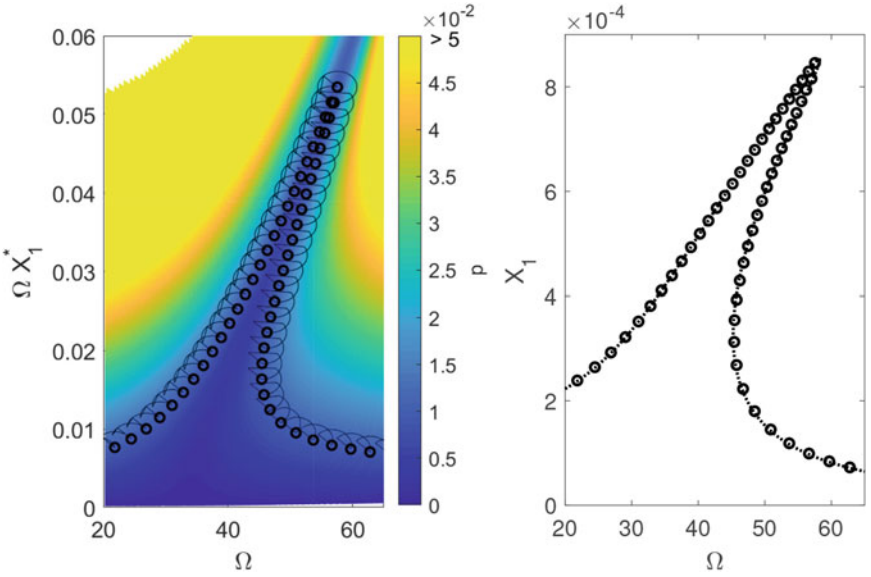

Fig. 16.7 Arclength continuation of a cubic oscillator with arclength integral control. The accepted points are marked by circles. (**a**) Input parameter space and (**b**) FRC at $p = 0.01$ (harmonic balance in dotted curve)

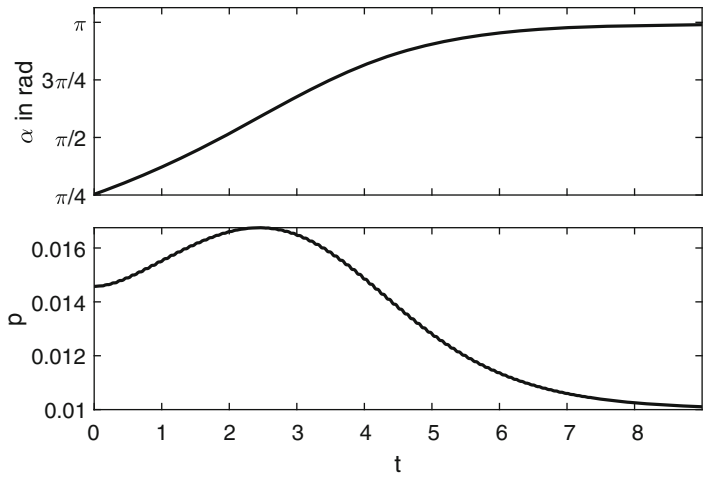

Fig. 16.8 Time series of the arc angle α (integral control) and force amplitude p along an arc centered at $\Omega X^* = 0.02$, $\Omega = 6.5$

The second arclength strategy is to use an integral controller acting on the arc angle α with the excitation amplitude error as the input, i.e., $\dot{\alpha} = k_\mathrm{i}(p - p^*)$. The path followed in Fig. 16.7 is similar to that in Fig. 16.4, because the arcs have the same dimensions. The effects of the transients are, however, diminished as the arc angle gently converges toward its target, as displayed in Fig. 16.8. The identified FRC in Fig. 16.7 is thus more accurate.

The influence of the integral gain k_i is similar to that of the sweep rate η_α. For instance, decreasing k_i leads to a longer (Table 16.4) but more accurate experiment (Fig. 16.9). Figure 16.9 evidences one drawback of the integral controller, namely, the arclength evolution depends on the force amplitude error. Input parameters further away from the desired values mean a greater force amplitude error and therefore faster evolution of the arclength. Decreasing the semi-major axes causes the experiment to last much longer (Table 16.4), but leads to excellent accuracy (Fig. 16.9). We note that a PID controller could also be considered. In theory, the proportional and differential gains could decrease the settling time and the overshoot. However, we think that a single control law cannot be optimal for the identification of the complete FRC, because the settling time would increase far away from resonance, whereas the overshoot would increase close to resonance.

The third arclength strategy combines both arc sweep and integral control. The arc is first swept at a constant rate η_α. This has the advantage that the arc's semi-major axes are decoupled from the rate at which the arclength evolves. When p^* is reached, the sweep is interrupted, and an integral controller is activated, allowing a gentle convergence toward p^*. Figure 16.10 plots the results for this strategy.

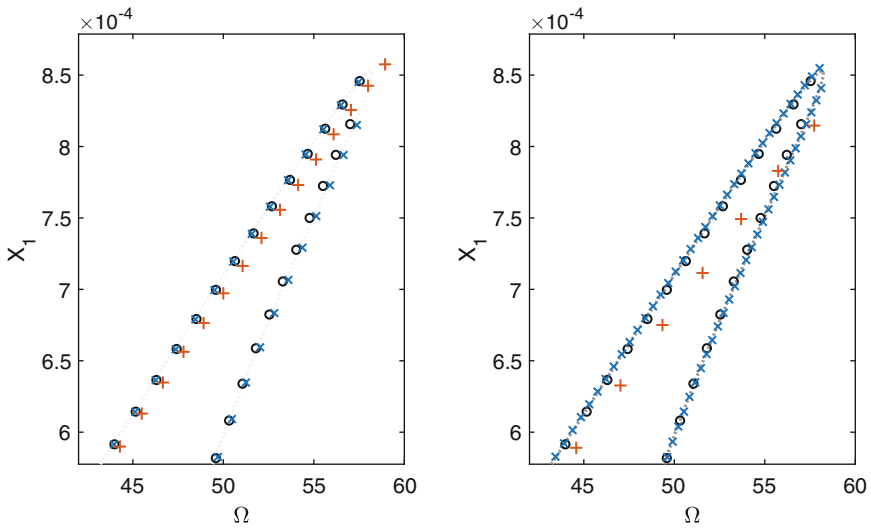

Fig. 16.9 Parametric study varying (**a**) the integral gain $k_\mathrm{i} = 40$ (blue $\times$), 75 (black $\circ$), and 150 (orange $+$) or (**b**) the semi-major axes $(\Delta\Omega, \Delta X^*) = (0.25, 0.001)$ (blue $\times$), $(0.5, 0.002)$ (black $\circ$), and $(1, 0.004)$ (orange $+$). The dotted curve represents harmonic balance results

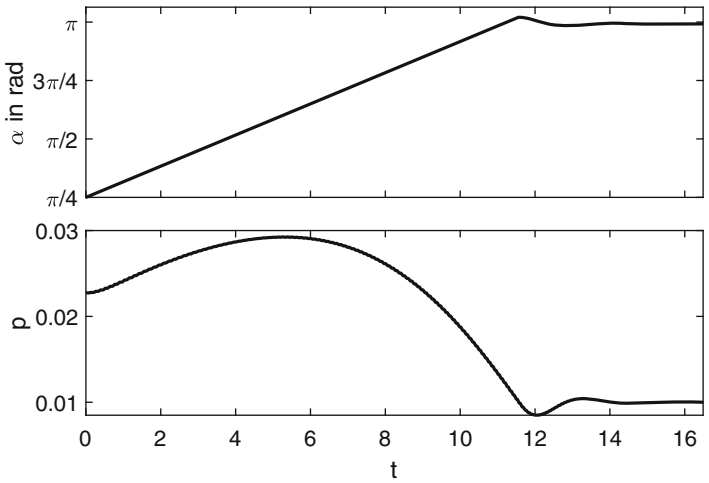

Fig. 16.10 Time series of the arc angle α (arc sweep+integral control) and force amplitude p along an arc centered at $\Omega X^* = 0.02$, $\Omega = 6.5$

16.3 Conclusion

This paper has introduced a novel experimental continuation method for FRCs requiring neither the estimation of derivatives nor the approximation of the response surface. One underlying assumption is that the input parameter space has no more than two dimensions. At the root of the method is an arclength continuation process during which the experiment follows an elliptic arc (centered on a previously identified response on the FRC) until it intersects the FRC again. Thanks to adaptive filtering, the continuation does not need to be halted, rendering the complete process fully online. The arclength continuation procedure was successfully validated numerically using a Duffing oscillator.

Acknowledgments The authors are grateful to « FONDS POUR LA FORMATION A LA RECHERCHE DANS L'INDUSTRIE ET DANS L'AGRICULTURE » (FRIA) for the financial support of G. Abeloos' thesis.

References

1. Riks, E.: An incremental approach to the solution of snapping and buckling problems. Int. J. Solids Struct. **15**, 529–551 (1979)
2. Crisfield, M.A.: A fast incremental/iterative solution procedure that handles "snap-through" (1981)
3. Abeloos, G., Renson, L., Kerschen, G.: Stepped and swept control-based continuation using adaptive filtering. Nonlinear Dyn. **104**, 3793–3808 (2021)